








Proceeding Paper

# Synthesis, Insecticidal Activity and Computational Studies of Eugenol-Based Insecticides <sup>†</sup>

José Ricardo A. Coelho <sup>1</sup>, Tatiana F. Vieira <sup>2,3</sup>, Renato B. Pereira <sup>4</sup>, David M. Pereira <sup>4</sup>,  
Elisabete M. S. Castanheira <sup>5,6</sup>, António Gil Fortes <sup>1</sup>, Sérgio F. Sousa <sup>2,3</sup>, Maria José G. Fernandes <sup>1</sup>  
and Maria Sameiro T. Gonçalves <sup>1,\*</sup>

- <sup>1</sup> Centre of Chemistry (CQ/UM), University of Minho, Campus of Gualtar, 4710-057 Braga, Portugal  
<sup>2</sup> Associate Laboratory i4HB—Institute for Health and Bioeconomy, Faculty of Medicine, University of Porto, 4200-319 Porto, Portugal  
<sup>3</sup> UCIBIO—Applied Molecular Biosciences Unit, BioSIM—Department of Biomedicine, Faculty of Medicine, University of Porto, Alameda Prof. Hernâni Monteiro, 4200-319 Porto, Portugal  
<sup>4</sup> REQUIMTE/LAQV, Laboratory of Pharmacognosy, Department of Chemistry, Faculty of Pharmacy, University of Porto, R. Jorge Viterbo Ferreira 228, 4050-313 Porto, Portugal  
<sup>5</sup> Physics Centre of Minho and Porto Universities (CF-UM-UP), University of Minho, Campus of Gualtar, 4710-057 Braga, Portugal  
<sup>6</sup> Associate Laboratory LaPMET—Laboratory of Physics for Materials and Emergent Technologies, University of Minho, Campus of Gualtar, 4710-057 Braga, Portugal  
\* Correspondence: msameiro@quimica.uminho.pt  
<sup>†</sup> Presented at the 26th International Electronic Conference on Synthetic Organic Chemistry, 15–30 November 2022; Available online: <https://sciforum.net/event/ecsoc-26>.

**Abstract:** Eugenol, a natural phenolic allyl benzene that has been used as an active lead compound showing significant biological activities, including insecticidal effects on a wide variety of domestic arthropod pests, was used as the main reagent in the present work. Ester eugenol derivatives were synthesized and evaluated for their insecticidal activities against the *Spodoptera frugiperda* cell line. Studies of structure-based inverted virtual screening were carried out in order to identify the potential targets associated with the obtained insecticidal activity. The results indicate that the insecticide activity observed is most likely a result of the interaction of these molecules with the odorant-binding proteins and/or with acetylcholinesterase.

**Keywords:** eugenol; eugenol esters; *Spodoptera frugiperda*; insecticides; computational studies



**Citation:** Coelho, J.R.A.; Vieira, T.F.; Pereira, R.B.; Pereira, D.M.; Castanheira, E.M.S.; Fortes, A.G.; Sousa, S.F.; Fernandes, M.J.G.; Gonçalves, M.S.T. Synthesis, Insecticidal Activity and Computational Studies of Eugenol-Based Insecticides. *Chem. Proc.* **2022**, *12*, 46. <https://doi.org/10.3390/ecsoc-26-13649>

Academic Editor: Julio A. Seijas

Published: 16 November 2022



**Copyright:** © 2022 by the authors. Licensee MDPI, Basel, Switzerland. This article is an open access article distributed under the terms and conditions of the Creative Commons Attribution (CC BY) license (<https://creativecommons.org/licenses/by/4.0/>).

## 1. Introduction

The global population is increasing at an exponential rate, so it is necessary to ensure agricultural production that meets the actual food requirements. In crop protection, the reduction in damage caused by pathogens and pests in agricultural fields is mainly achieved through the extensive use of synthetic pesticides. To mitigate the environmental problems caused by the intensive use of conventional synthetic pesticides, biopesticides and semi-synthetic pesticides based on natural plant products are alternatives as pest-management agents [1,2].

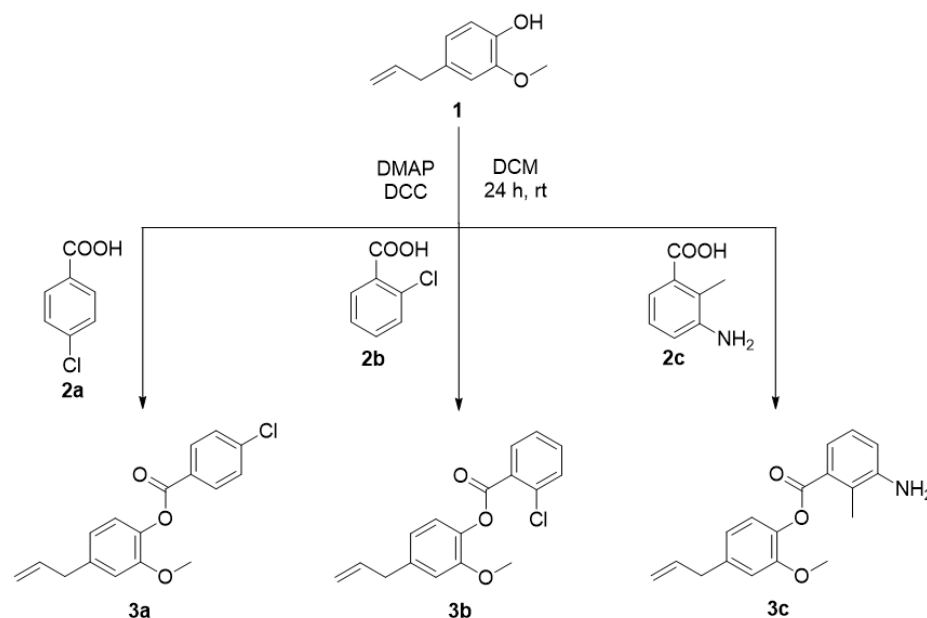
Natural products are good substrates, due to their structural diversity and associated biological activity. Among several groups of natural insecticides (pyrethroids, neonicotinoids, avermectins, etc.), essential oils and their derivatives have also shown relevant potential as insecticides [3–5]. One possibility is eugenol, 4-allyl-2-methoxyphenol, a volatile phenolic bioactive compound that has been identified in several aromatic plants, among them *Syzygium aromaticum*, and has shown a wide range of biological activities including anti-inflammatory, antioxidant, analgesic, anticancer, antifungal, antimicrobial, antiparasitic and insecticidal activities [6–11].

Considering these facts, in the present work, eugenol derivatives were synthesized through an esterification reaction and evaluated for their effect on the viability of *Sf9* cells. A structure-based inverted virtual screening protocol was employed to identify the potential proteins associated with the observed insecticidal activity.

## 2. Results and Discussion

### 2.1. Synthesis of Compounds 3a–c

The reaction of eugenol, the trivial name for 4-allyl-2-methoxyphenol **1**, with 4-chlorobenzoic acid **2a**, 2-chlorobenzoic acid **2b** and 3-amino-2-methylbenzoic acid **2c** in dichloromethane, at room temperature and in the presence of 4-dimethylaminopyridine (DMAP) and *N,N'*-dicyclohexylcarbodiimide (DCC) gave the corresponding ester derivatives, namely 4-allyl-2-methoxyphenyl 4-chlorobenzoate **3a**, 4-allyl-2-methoxyphenyl 2-chlorobenzoate **3b** and 4-allyl-2-methoxyphenyl 3-amino-2-methylbenzoate **3c**, respectively (Scheme 1). All compounds were obtained in 46% to 56% yields, and were characterized with the usual analytical techniques.



**Scheme 1.** Synthesis of esters derived from eugenol **3a–c**.

The  $^1\text{H}$  NMR of compounds **3a–c** show the signals of aromatic protons derived from the 4-allyl-2-methoxyphenyl group ( $\delta$  6.80–7.10 ppm) in addition to the protons of 4-chloro-, 2-chloro- or 3-amino-2-methylbenzoate, highlighting H-5 and H-6 displayed as doublets, double doublets or double triplets ( $\delta$  7.28–7.49 ppm, H-5;  $\delta$  7.86–8.16 ppm, H-6). The alkene protons are shown as multiplets ( $\delta$  5.10–5.17 and 5.95–6.05 ppm). The  $^{13}\text{C}$  NMR show the signals related to ester bonds ( $\delta$  164.08–165.68 ppm) in all compounds. The IR spectra also confirm the presence of the ester bonds through the stretching vibration bands of the carbonyl groups ( $\nu$  1718 to 1748  $\text{cm}^{-1}$ ).

### 2.2. Biological Activity of Compounds 3a–c

The impact of ester eugenol derivatives **3a–c** on the viability of *Sf9* cells was evaluated at 100  $\mu\text{g/mL}$ , following 24 h of exposure. As shown in Figure 1, compounds **3a** and **3b**, resulting from the eugenol esterification with chlorobenzoic acids, displayed similar toxicity to the starting material eugenol **1**. On the other hand, the eugenol esterification with 3-amino-2-methylbenzoic acid led to increased activity (compound **3c**), causing nearly 50% of viability loss.

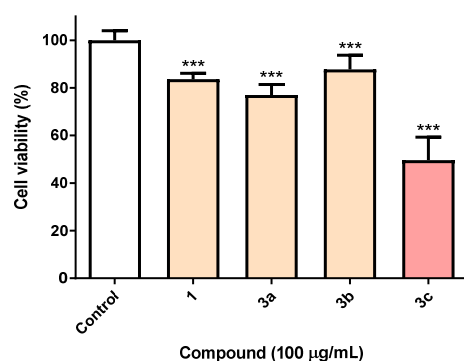


**Figure 1.** Viability of *Sf9* cells after incubation with the indicated molecules (100 µg/mL). \*\*\*  $p < 0.001$ .

### 2.3. Inverted Virtual Screening Results

In Table 1, the average score for all the eugenol derivatives is presented for each potential target using each scoring function. In each set of targets, the structure with the highest score was selected and ranked from best to worst, based on the docking programs/scoring functions' predictions. For this study, the four scoring functions (SFs) of GOLD were used. The score of each of the GOLD SFs is dimensionless, with a higher value indicating a better binding affinity.

**Table 1.** Average scores obtained with the five different scoring functions used and overall ranking.

Target	PDB	PLP	ASP	ChemScore	GoldScore	Overall Ranking
Acetylcholinesterase	1QON	79.20	52.57	38.45	63.13	2
	4EY6	76.48	46.52	37.82	44.88	
	1DX4	74.00	46.63	39.16	60.42	
Alpha-esterase-7 ( $\alpha$ E7)	5TYJ	66.80	38.34	34.30	57.03	6
	5TYP	64.80	39.40	34.36	55.56	
Beta-N-acetyl-D-hexosaminidase of Hex1	3NSN	73.92	49.50	32.12	65.90	3
	3OZP	68.18	45.24	31.82	63.98	
Chitinase	3WL1	74.27	44.47	33.97	59.11	4
	3WQV	74.00	45.92	34.03	63.07	
Ecdysone receptor	1R20	71.27	33.41	34.24	57.75	5
	1R1K	67.57	33.21	36.12	59.70	
<i>N</i> -Acetylglucosamine-1-phosphate uridyltransferase (GlmU)	2V0K	55.34	24.38	22.77	54.47	13
	2VD4	47.33	26.02	24.36	47.33	
Octopamine receptor	4N7C	60.62	32.69	33.20	55.29	10
Odorant-binding protein	5V13	82.14	48.95	39.88	66.73	1
	2GTE	77.42	46.50	42.19	68.77	
	3N7H	76.75	39.81	31.76	70.47	
	3K1E	67.38	39.88	37.26	61.61	
Peptide deformylase	5CY8	67.11	30.00	25.58	64.72	7
<i>p</i> -hydroxyphenylpyruvate dioxygenase	6ISD	63.14	37.74	28.09	55.42	8
Polyphenol oxidase	1BUG	52.80	31.50	22.15	58.42	12
Sterol carrier protein-2 (HaSCP-2)	4UEI	62.77	32.80	33.39	52.06	9
Voltage-gated sodium channel	6A95	58.26	23.58	23.60	59.52	11

There is a high degree of consistency across all SFs, with odorant-binding proteins (OBPs) and acetylcholinesterases (AChEs) suggesting more likely binding. The octopamine

receptor, voltage-gated sodium channel, polyphenol oxidase and *N*-acetylglucosamine-1-phosphate uridylyltransferase (GlmU) consistently exhibit lower scores.

#### 2.4. Molecular Dynamics Simulations and Free Energy Calculation Results

Simulations were carried out for both groups of targets predicted at the inverted VS stage odorant binding proteins and acetylcholinesterases, in complex with the three most potent eugenol derivatives. The structures chosen were the ones that presented the best score from each group (3K1E for OBP and 1QON for acetylcholinesterases—AChE). Molecular dynamics simulations were used to confirm and validate the inverted screening predictions, allowing for a more detailed analysis. Additionally, the interactions formed between the protein and ligand were further analyzed, and the most determinant residues were identified. The results are presented in Table 2.

The protein RMSD value of OBP compared to the docking pose had an average value of about 2.3 Å. Interestingly, the AChE complexes presented a higher RMSD value. However, in these cases, the standard deviation was low. It is possible that the complexes of AChE and the eugenol derivatives were optimized at the beginning of the simulation to obtain a more stable conformation. Throughout the simulation, all molecules remained bound to their targets and an induced-fit adjustment was observed. A study was also conducted to determine how buried the eugenol derivatives were in the binding pockets, measuring the solvent accessible surface area (SASA) and the percentage of potential SASA. An increase in the percentage of ligand SASA with a lower SASA indicates that the molecule is buried in the target pocket, making it less exposed to solvent. Compound **3b** is the most buried in the OBP pocket (with a percentage of ligand SASA of 97% and an average SASA of 18.5 Å<sup>2</sup>). Regarding AChE, compound **3a** is the most buried in the active site (with a percentage of ligand SASA of 94% and a SASA of 31.7 Å<sup>2</sup>).

The three eugenol derivatives exhibit slightly better binding affinities toward OBP, with compound **3a** showing a  $\Delta G_{\text{bind}}$  of −35.6 kcal/mol when in complex with OBP and −33.5 kcal/mol when bound to AChE. When compared to the other compounds, compound **3c** is the weakest binder for both OBP and AChE (with  $\Delta G_{\text{bind}}$  of −30.1 kcal/mol when bound to OBP and −29.1 kcal/mol when bound to AChE).

When bound to OBP, the compounds are stabilized primarily by electrostatic interactions with Trp114, Leu76, Gly92, Phe15, Leu80 and Tyr122. From all the compounds studied, the results seem to suggest that compounds **3a** and **3b** may be good candidates to be used as repellents, having OBP as their main target. Regarding AChE, the main interacting residues are Tyr71, Trp83 and Tyr374.

**Table 2.** Average RMSD values (Å), ligand RMSD (Å), average SASA (Å<sup>2</sup>), percentage of potential ligand SASA buried and average number of hydrogen bonds for the ligands for the last 70 ns of the simulation of the OBP and AChE–ligand complexes.

		Average RMSD of the Complex (Å)	Average RMSD of the Ligand (Å)	Average SASA (Å <sup>2</sup> )	Percentage of Potential Ligand SASA Buried (%)	Average Number of H Bonds	$\Delta G_{\text{bind}}$ (kcal/mol)	Main Contributors
OBP	<b>3a</b>	2.5 ± 0.2	0.6 ± 0.3	65.1 ± 13.7	87	0.01 ± 0.07	−35.6 ± 0.2	Trp114 (−2.7 ± 0.5) Leu76 (−1.9 ± 0.5) Gly92 (−1.5 ± 0.5)
	<b>3b</b>	2.1 ± 0.3	1.3 ± 0.4	18.5 ± 10.6	97	0.01 ± 0.1	−32.1 ± 0.2	Trp114 (−1.3 ± 0.4) Phe15 (−1.2 ± 0.3) Leu80 (−1.2 ± 0.3)
	<b>3c</b>	2.4 ± 0.3	1.5 ± 0.4	30.1 ± 17.0	94	0.1 ± 0.2	−30.1 ± 0.2	Met19 (−1.5 ± 0.5) Phe59 (−1.3 ± 0.5) Tyr122 (−1.3 ± 0.4)
AChE	<b>3a</b>	3.2 ± 0.4	0.5 ± 0.2	31.7 ± 12.2	94	0.4 ± 0.5	−33.5 ± 0.1	Trp83 (−2.4 ± 0.5) Tyr71 (−1.4 ± 0.4) Tyr374 (−1.2 ± 0.4)
	<b>3b</b>	4.0 ± 0.7	0.9 ± 0.2	74.2 ± 37.4	85	0.1 ± 0.2	−25.5 ± 0.2	Tyr71 (−1.5 ± 0.7) Tyr374 (−1.0 ± 0.4) Trp83 (−1.9 ± 0.8)
	<b>3c</b>	3.1 ± 0.3	0.9 ± 0.2	47.6 ± 22.1	91	0.4 ± 0.6	−29.1 ± 0.2	Tyr71 (−1.5 ± 0.5) Tyr374 (−1.4 ± 0.9)

### 3. Material and Methods

#### 3.1. Typical Procedure for the Preparation of Compounds 3a–c (Illustrated for 3a)

A mixture of 4-allyl-2-methoxyphenol **1** (0.500 g, 3.05 mmol), DMAP (0.075 g, 0.61 mmol) and DCC (0.944 g, 4.56 mmol) was added to a solution of 4-chlorobenzoic acid **2a** (0.716 g, 4.58 mmol) in dichloromethane (5 mL). The reaction mixture was stirred for 24 h at room temperature and was monitored by TLC (silica: dichloromethane). The white suspension obtained was filtered and the liquid phase was washed successively with 5% (*w/v*) HCl (2 × 5 mL), 5% NaHCO<sub>3</sub> (*w/v*; 3 × 5 mL) and H<sub>2</sub>O (3 × 5 mL). After drying with anhydrous MgSO<sub>4</sub>, the organic phase was evaporated under reduced pressure. Compound **3a** was obtained as a yellow solid (0.523 g; 56%). *R*<sub>f</sub> = 0.61 (silica: dichloromethane), m.p. = 76–78 °C. IR ( $\nu_{\max}$ ): 3306, 2934, 1737, 1646, 1591, 1506, 1487, 1464, 1421, 1401, 1284, 1262, 1198, 1187, 1172, 1149, 1068, 922, 847, 751, 732 cm<sup>−1</sup>. <sup>1</sup>H NMR (CDCl<sub>3</sub>, 400 MHz):  $\delta_{\text{H}}$  3.42 (2H, d, *J* = 6.8 Hz, CH<sub>2</sub>Ph), 3.81 (3H, s, OCH<sub>3</sub>), 5.10–5.17 (2H, m, CH=CH<sub>2</sub>), 5.95–6.05 (1H, m, CH=CH<sub>2</sub>), 6.82 (1H, d, *J* = 1.6 Hz, H-2), 6.84 (1H, dd, *J* = 6.0 and 1.6 Hz, H-5), 7.07 (1H, d, *J* = 8.0 Hz, H-6), 7.49 (2H, d, *J* = 8.8 Hz, H-3 and H-5 Ph-Cl), 8.16 (2H, d, *J* = 8.8 Hz, H-2 and H-6 Ph-Cl) ppm. <sup>13</sup>C NMR (CDCl<sub>3</sub>, 100 MHz):  $\delta_{\text{C}}$  40.09 (CH<sub>2</sub>Ph), 55.84 (OCH<sub>3</sub>), 112.82 (C-3), 116.17 (CH=CH<sub>2</sub>), 120.72 (C-6), 122.52 (C-5), 127.95 (C-1 Ph-Cl), 128.82 (C-3 and C-5 Ph-Cl), 131.65 (C-2 and C-6 Ph-Cl), 137.01 (CH=CH<sub>2</sub>), 137.99 (C-4), 139.20 (C-4 Ph-Cl) 139.88 (C-1), 150.97 (C-2), 164.08 (C=O) ppm.

#### 3.2. Biological Assays

The potential of compounds **3a–c** as biopesticides was evaluated in assays using the *Sf9* (*Spodoptera frugiperda*) insect cell line. Cells were maintained at 28 °C and cultivated in Grace's medium with 10% FBS. For the evaluation of viability, cells were plated at 3.0 × 10<sup>4</sup> cells/well and exposed to the molecules, after which resazurin was added, and the fluorescence was read at 560/590 nm after 60 min of incubation.

#### 3.3. Docking and Inverted Virtual Screening Studies

The Scopus database was searched for papers reporting virtual screening studies involving targets and molecules with insecticidal activity. The publication year and relevance of the target were considered in the selection process. A total of thirteen targets were identified in the eighteen studies found, as shown in Table 3.

**Table 3.** List of targets selected for the inverted virtual screening study.

Target	Organism	PDB Target	Resolution (Å)	Ref.
Acetylcholinesterase	<i>Aedes aegypti</i>	1QON	2.72	[12]
		4EY6	2.40	
	<i>Drosophila melanogaster</i>	1DX4	2.70	[13]
Alpha-esterase-7 (αE7)	<i>Lucilia cuprina</i>	5TYJ	1.75	[14]
		5TYP	1.88	
beta-N-acetyl-D-hexosaminidase OfHex1	<i>Ostrinia furnacalis</i>	3NSN	2.10	[15]
		3OZP	2.00	[16]
		3WL1	1.77	
Chitinase	<i>Ostrinia furnacalis</i>	3WQV	2.04	[17]
		1R20	3	
Ecdysone receptor	<i>Heliothis virescens</i>	1R1K	2.9	[19]
		2V0K	2.3	
N-Acetylglucosamine-1-phosphate uridylyltransferase (GlmU)	<i>Xanthomonas oryzae</i>	2VD4	1.9	[20]
		4N7C	1.75	
Octopamine receptor	<i>Blattella germanica</i>	5V13	1.84	[12]
	<i>Aedes aegypti</i>	2GTE	1.4	
	<i>Drosophila melanogaster</i>	3N7H	1.6	
Odorant-binding protein	<i>Anopheles gambiae</i>	3K1E	1.85	[23]
	<i>Aedes aegypti</i>	5CY8	2.38	
	<i>Xanthomonas oryzae</i>	6ISD	2.4	
Peptide deformylase	<i>Arabidopsis thaliana</i>	3HSS	2.7	[24]
p-hydroxyphenylpyruvate dioxygenase	<i>Manduca sexta</i>	4UEI	Solution NMR	[25]
Polyphenol oxidase	<i>Helicoverpa armigera</i>	6A95	2.6	[26]
Sterol carrier protein-2 (HaSCP-2)	<i>Periplaneta americana</i>			[27]
Voltage-gated sodium channel				[28]

After preparing each PDB structure (removing water and other molecules from the crystallization process), the crystallographic ligands were extracted and saved in separate files, to provide a reference site for docking coordinates and to posteriorly perform re-docking. In the absence of crystallographic ligands, active site residues were selected based on their importance for activity. In order to evaluate the quality of the docking protocol, as well as the capability of the docking software to reproduce geometry and orientation of the crystallographic pose, re-docking was used. The docking program/scoring functions used was GOLD [29] (PLP, ASP, ChemScore and GoldScore). By comparing the predicted docking pose with the crystallographic one through RMSD calculation, the ability of the SF to correctly dock the ligand is evaluated and that is a valuable step in the validation process. A lower RMSD means a better docking prediction.

The three eugenol derivatives were prepared for the study using DataWarrior [30] and OpenBabel [31], and subsequently docked into each PDB structure, using all the four SFs as soon as the protocol was optimized. The parameters that were optimized for each program/scoring function were: the docking coordinates, the docking box dimension or radius, the exhaustiveness, the search efficiency and the number of runs. Lastly, a ranked list was prepared based on the average scores of each target.

### 3.4. Molecular Dynamics Simulations and Free Energy Calculations

The three eugenol derivatives (compounds **3a**, **3b** and **3c**) in complex with the two most promising targets identified from the inverted virtual screening study (odorant-binding protein 1—3KIE and acetylcholinesterase—1QON) were further studied through 100 ns molecular dynamics simulations with the Amber18 software [32].

The pose predicted at the IVS stage (with the PLP scoring function) was selected as the starting point of each MD simulation. ANTECHAMBER with RESP HF/6-31G(d) charges (calculated with Gaussian16 [33] and the general Amber force field (GAFF) [34]) were used to assign parameters. To describe the protein targets, the ff14SB force field [35] was applied. Posteriorly, the protein–ligand complexes were placed in TIP3P water boxes with a minimum distance of 12 Å between the protein surface and the side of the box, and periodic boundary conditions were used. By adding counter-ions ( $\text{Na}^+$ ), the overall charge on the system was neutralized. Ewald's particle-mesh summation method was used to calculate long-range electrostatic interactions, while for short-range electrostatic and Lennard-Jones interactions, a cut-off value of 10.0 Å was used. A time step of 2 fs was used and all bonds involving hydrogen atoms were constrained using the SHAKE algorithm.

Then, the systems were submitted to four consecutive minimization stages to remove clashes, followed by an equilibration and production run, with each minimization having a maximum of 2500 cycles. In the equilibration run, the procedure was divided into two phases; NVT ensemble, where the systems were gradually heated to 298 K using a Langevin thermostat at constant volume (50 ps), and equilibration of the system density at 298 K (subsequent 50 ps). Lastly, the production run was performed during 100 ns with an NPT ensemble at constant temperature (298 K, Langevin thermostat) and pressure (1 bar, Berendsen barostat). The last 70 ns of the simulation were considered for SASA and hydrogen bonding analysis.

In this study, the molecular mechanics/generalized Born surface area method [36] was used in conjunction with the MM/PBSA.py script [37] from Amber. Each simulation's last 70 ns were analyzed with an interval of 100 ps and salt concentration of 0.100 mol dm<sup>−3</sup>. Additionally, the contribution of the amino acid residues was evaluated using the energy decomposition method. The MM-GBSA calculations considered 1400 conformations from each MD trajectory taken from the last 70 ns of simulation.

## 4. Conclusions

The eugenol derivatives obtained were fully characterized and their biological evaluation as insecticides using the *Sf9* (*Spodoptera frugiperda*) insect cell line has shown that it was possible to obtain a molecule (compound **3c**) that was more toxic by tuning its structure.



The results strongly suggest that the insecticide activity observed arises from their interaction with the odorant-binding proteins and/or with acetylcholinesterase.

**Author Contributions:** Conceptualization, M.J.G.F., D.M.P., M.S.T.G. and S.F.S.; methodology, J.R.A.C., M.S.T.G., S.F.S., E.M.S.C. and D.M.P.; formal analysis, J.R.A.C., M.S.T.G., M.J.G.F., R.B.P., D.M.P. and S.F.S.; investigation, J.R.A.C., T.F.V. and R.B.P.; validation, M.J.G.F., D.M.P., M.S.T.G., E.M.S.C., S.F.S. and M.S.T.G.; writing—original draft preparation, J.R.A.C., M.S.T.G., M.J.G.F., R.B.P. and S.F.S.; writing—review and editing, M.S.T.G., M.J.G.F., R.B.P., D.M.P., S.F.S. and E.M.S.C.; supervision, M.S.T.G., M.J.G.F. and A.G.F.; project administration, M.S.T.G. All authors have read and agreed to the published version of the manuscript.

**Funding:** This research was funded by FCT under project PTDC/ASP-AGR/30154/2017 (PO-CI-01-0145-FEDER-030154) of COMPETE 2020, co-financed by FEDER and the EU. FCT-Portugal and FEDER-COMPETE/QREN-EU also gave financial support to the research centers CQ/UM (UIDB/00686/2021), CF-UM-UP (UIDB/04650/2021) and REQUIMTE (UIDB/50006/2021). The NMR spectrometer Bruker Avance III 400 (part of the National NMR Network) was financed by FCT and FEDER.

**Institutional Review Board Statement:** Not applicable.

**Informed Consent Statement:** Not applicable.

**Data Availability Statement:** Not applicable.

**Conflicts of Interest:** The authors declare no conflict of interest.

## References

1. Liu, X.; Cao, A.; Yan, D.; Ouyang, C.; Wang, Q.; Li, Y. Overview of mechanisms and uses of biopesticides. *Int. J. Pest Manag.* **2021**, *67*, 65–72. [\[CrossRef\]](#)
2. Lengai, G.M.W.; Muthomi, J.W.; Mbega, E.R. Phytochemical activity and role of botanical pesticides in pest management for sustainable agricultural crop production. *Sci. Afr.* **2020**, *7*, e00239. [\[CrossRef\]](#)
3. Salman, M.; Abbas, R.Z.; Israr, M.; Abbas, A.; Mehmood, K.; Khan, M.K.; Sindhu, Z.D.; Hussain, R.; Saleem, M.K.; Shaha, S. Repellent and acaricidal activity of essential oils and their components against *Rhipicephalus* ticks in cattle. *Vet. Parasitol.* **2020**, *283*, 109178. [\[CrossRef\]](#) [\[PubMed\]](#)
4. Chaieb, K.; Hajlaoui, H.; Zmantar, T.; Ben Kahla-Nakbi, A.; Rouabhia, M.; Mahdouani, K.; Bakhrouf, A. The chemical composition and biological activity of clove essential oil, *Eugenia Caryophyllata* (*Syzygium Aromaticum* L. *Myrtaceae*): A short review. *Phytother. Res.* **2007**, *21*, 501–506. [\[CrossRef\]](#) [\[PubMed\]](#)
5. Natal, C.M.; Fernandes, M.J.G.; Pinto, N.F.S.; Pereira, R.B.; Vieira, T.F.; Rodrigues, A.R.O.; Pereira, D.M.; Sousa, S.F.; Fortes, A.G.; Castanheira, E.M.S.; et al. New carvacrol and thymol derivatives as potential insecticides: Synthesis, biological activity, computational studies and nanoencapsulation. *RSC Adv.* **2021**, *11*, 34024–34035. [\[CrossRef\]](#)
6. Ju, J.; Xie, Y.; Yu, H.; Guo, Y.; Cheng, Y.; Qian, H.; Yao, W. Analysis of the synergistic antifungal mechanism of eugenol and citral. *LWT Food Sci. Technol.* **2020**, *123*, 109128. [\[CrossRef\]](#)
7. Lee, M.Y. Essential oils as repellents against arthropods. *Biomed. Res. Int.* **2018**, *2018*, 6860271. [\[CrossRef\]](#)
8. Fernandes, M.J.G.; Pereira, R.B.; Pereira, D.M.; Fortes, A.G.; Castanheira, E.M.S.; Gonçalves, M.S.T. New eugenol derivatives with enhanced insecticidal activity. *Int. J. Mol. Sci.* **2020**, *21*, 9257. [\[CrossRef\]](#)
9. Pereira, R.B.; Pinto, N.F.S.; Fernandes, M.J.G.; Vieira, T.F.; Rodrigues, A.R.O.; Pereira, D.M.; Sousa, S.F.; Castanheira, E.M.S.; Fortes, A.G.; Gonçalves, M.S.T. Amino alcohols from eugenol as potential semisynthetic insecticides: Chemical, biological and computational insights. *Molecules* **2021**, *26*, 6616. [\[CrossRef\]](#)
10. Coelho, C.M.M.; Pereira, R.B.; Vieira, T.F.; Teixeira, C.M.; Fernandes, M.J.G.; Rodrigues, A.R.O.; Pereira, D.M.; Sousa, S.F.; Fortes, A.G.; Castanheira, E.M.S.; et al. Synthesis, computational and nanoencapsulation studies on eugenol-derived insecticides. *New J. Chem.* **2022**, *46*, 14375–14387. [\[CrossRef\]](#)
11. Fernandes, M.J.G.; Pereira, R.B.; Rodrigues, A.R.O.; Vieira, T.F.; Fortes, A.G.; Pereira, D.M.; Sousa, S.F.; Gonçalves, M.S.T.; Castanheira, E.M.S. Liposomal formulations loaded with an eugenol derivative for application as insecticides: Encapsulation studies and in silico identification of protein targets. *Nanomaterials* **2022**, *12*, 3583. [\[CrossRef\]](#) [\[PubMed\]](#)
12. Ramos, R.S.; Costa, J.S.; Silva, R.C.; Costa, G.V.; Rodrigues, A.B.L.; Rabelo, E.M.; Souto, R.N.P.; Taft, C.A.; Silva, C.H.T.P.; Rosa, J.M.C.; et al. Identification of potential inhibitors from Pyriproxyfen with insecticidal activity by virtual screening. *Pharmaceuticals* **2019**, *12*, 20. [\[CrossRef\]](#) [\[PubMed\]](#)
13. Riva, C.; Suzanne, P.; Charpentier, G.; Dulin, F.; Halm-Lemeille, M.P.; Sopkova-de Oliveira Santos, J. In silico chemical library screening and experimental validation of novel compounds with potential varroacide activities. *Pestic. Biochem. Physiol.* **2019**, *160*, 11–19. [\[CrossRef\]](#) [\[PubMed\]](#)



14. Correy, G.J.; Zaidman, D.; Harmelin, A.; Carvalho, S.; Mabbitt, P.D.; Viviane, C.; James, P.J.; Kotze, A.C.; Jackson, C.J.; London, N. Overcoming insecticide resistance through computational inhibitor design. *Proc. Natl. Acad. Sci. USA* **2019**, *116*, 21012–21021. [\[CrossRef\]](#)
15. Liu, J.; Liu, M.; Yao, Y.; Wang, J.; Li, Y.; Li, G.; Wang, Y. Identification of novel potential  $\beta$ -N-acetyl-D-hexosaminidase inhibitors by virtual screening, molecular dynamics simulation and MM-PBSA calculations. *Int. J. Mol. Sci.* **2012**, *13*, 4545–4563. [\[CrossRef\]](#)
16. Dong, L.; Shen, S.; Xu, Y.; Wang, L.; Yang, Q.; Zhang, J.; Lu, H. Identification of novel insect  $\beta$ -N-acetylhexosaminidase OffHex1 inhibitors based on virtual screening, biological evaluation, and molecular dynamics simulation. *J. Biomol. Struct. Dyn.* **2021**, *39*, 1735–1743. [\[CrossRef\]](#)
17. Dong, Y.; Jiang, X.; Liu, T.; Ling, Y.; Yang, Q.; Zhang, L.; He, X. Structure-based virtual screening, compound synthesis, and bioassay for the design of chitinase inhibitors. *J. Agric. Food Chem.* **2018**, *66*, 3351–3357. [\[CrossRef\]](#)
18. Hu, X.; Yin, B.; Cappelle, K.; Swevers, L.; Smaghe, G.; Yang, X.; Zhang, L. Identification of novel agonists and antagonists of the ecdysone receptor by virtual screening. *J. Mol. Graph. Model.* **2018**, *81*, 77–85. [\[CrossRef\]](#)
19. Harada, T.; Nakagawa, Y.; Ogura, T.; Yamada, Y.; Ohe, T.; Miyagawa, H. Virtual screening for ligands of the insect molting hormone receptor. *J. Chem. Inf. Model.* **2011**, *51*, 296–305. [\[CrossRef\]](#)
20. Min, J.; Lin, D.; Zhang, Q.; Zhang, J.; Yu, Z. Structure-based virtual screening of novel inhibitors of the uridyltransferase activity of *Xanthomonas oryzae* pv. *oryzae* GlmU. *Eur. J. Med. Chem.* **2012**, *53*, 150–158. [\[CrossRef\]](#)
21. Offermann, L.R.; Chan, S.L.; Osinski, T.; Tan, Y.W.; Chew, F.T.; Sivaraman, J.; Mok, Y.K.; Minor, W.; Chruszcz, M. The major cockroach allergen Bla g 4 binds tyramine and octopamine. *Mol. Immunol.* **2014**, *60*, 86–94. [\[CrossRef\]](#) [\[PubMed\]](#)
22. Laughlin, J.D.; Ha, T.S.; Jones, D.N.M.; Smith, D.P. Activation of pheromone-sensitive neurons is mediated by conformational activation of pheromone-binding protein. *Cell* **2008**, *133*, 1255–1265. [\[CrossRef\]](#) [\[PubMed\]](#)
23. Oliferenko, P.V.; Oliferenko, A.A.; Poda, G.I.; Osolodkin, D.I.; Pillai, G.G.; Bernier, U.R.; Tsikolia, M.; Agramonte, N.M.; Clark, G.G.; Linthicum, K.J.; et al. Promising *Aedes aegypti* repellent chemotypes identified through integrated QSAR, virtual screening, synthesis, and bioassay. *PLoS ONE* **2013**, *8*, e64547. [\[CrossRef\]](#) [\[PubMed\]](#)
24. Joshi, T.; Joshi, T.; Sharma, P.; Chandra, S.; Pande, V. Molecular docking and molecular dynamics simulation approach to screen natural compounds for inhibition of *Xanthomonas oryzae* pv. *Oryzae* by targeting peptide deformylase. *J. Biomol. Struct. Dyn.* **2021**, *39*, 823–840. [\[CrossRef\]](#)
25. Fu, Y.; Liu, Y.X.; Kang, T.; Sun, Y.N.; Li, J.Z.; Ye, F. Identification of novel inhibitors of *p*-hydroxyphenylpyruvate dioxygenase using receptor-based virtual screening. *J. Taiwan Inst. Chem. Eng.* **2019**, *103*, 33–43. [\[CrossRef\]](#)
26. Fattouch, S.; Raboudi-Fattouch, F.; Ponce, J.V.; Forment, J.V.; Lukovic, D.; Marzouki, N.; Vidal, D.R. Concentration dependent effects of commonly used pesticides on activation versus inhibition of the quince (*Cydonia oblonga*) polyphenol oxidase. *Food Chem. Toxicol.* **2010**, *48*, 957–963. [\[CrossRef\]](#)
27. Cai, J.; Du, X.; Wang, C.; Lin, J.; Du, X. Identification of potential *Helicoverpa armigera* (Lepidoptera: Noctuidae) sterol carrier protein-2 inhibitors through high-throughput virtual screening. *J. Econ. Entomol.* **2017**, *110*, 1779–1784. [\[CrossRef\]](#)
28. Shen, H.; Li, Z.; Jiang, Y.; Pan, X.; Wu, J.; Cristofori-Armstrong, B.; Smith, J.J.; Chin, Y.K.Y.; Lei, J.; Zhou, Q.; et al. Structural basis for the modulation of voltage-gated sodium channels by animal toxins. *Science* **2018**, *362*, eaau2596. [\[CrossRef\]](#)
29. Jones, G.; Willett, P.; Glen, R.C.; Leach, A.R.; Taylor, R. Development and validation of a genetic algorithm for flexible docking 1, F.E. Cohen (Ed). *J. Mol. Biol.* **1997**, *267*, 727–748. [\[CrossRef\]](#)
30. Sander, T.; Freyss, J.; von Korff, M.; Rufener, C. Data warrior: An open-source program for chemistry aware data visualization and analysis. *J. Chem. Inf. Model.* **2015**, *55*, 460–473. [\[CrossRef\]](#)
31. O'Boyle, N.M.; Banck, M.; James, C.A.; Morley, C.; Vandermeersch, T.; Hutchison, G.R. Open Babel: An open chemical toolbox. *J. Cheminform.* **2011**, *3*, 33. [\[CrossRef\]](#)
32. Case, D.A.; Cheatham, T.E., 3rd; Darden, T.; Gohlke, H.; Luo, R.; Merz, K.M., Jr.; Onufrie, A.; Simmerling, C.; Wang, B.; Woods, R.J. The Amber biomolecular simulation programs. *J. Comput. Chem.* **2005**, *26*, 1668–1688. [\[CrossRef\]](#) [\[PubMed\]](#)
33. Frisch, M.J.; Trucks, G.; Schlegel, H.B.; Frisch, M.J.; Trucks, G.W.; Schlegel, H.B.; Scuseria, G.E.; Robb, M.A.; Cheeseman, J.R.; Scalmani, G.; et al. *Gaussian 09, Revision A.02*; Gaussian Inc.: Wallingford, CT, USA, 2016.
34. Wang, J.; Wolf, R.M.; Caldwell, J.W.; Kollman, P.A.; Case, D.A.; Wang, J. Development and testing of a general amber force field. *J. Comp. Chem.* **2004**, *25*, 1157–1174. [\[CrossRef\]](#) [\[PubMed\]](#)
35. Maier, J.A.; Martinez, C.; Kasavajhala, K.; Wickstrom, L.; Hauser, K.E.; Simmerling, C. ff14SB: Improving the accuracy of protein side chain and backbone parameters from ff99SB. *J. Chem. Theory Comput.* **2015**, *11*, 3696–3713. [\[CrossRef\]](#) [\[PubMed\]](#)
36. Wang, E.; Sun, H.; Wang, J.; Wang, Z.; Liu, H.; Zhang, J.Z.H.; Hou, T. End-point binding free energy calculation with MM/PBSA and MM/GBSA: Strategies and applications in drug design. *Chem. Rev.* **2019**, *119*, 9478–9508. [\[CrossRef\]](#) [\[PubMed\]](#)
37. Miller, B.R.; McGee, T.D.; Swails, J.M.; Homeyer, N.; Gohlke, H.; Roitberg, A.E. MMPBSA.py: An efficient program for end-state free energy calculations. *J. Chem. Theory Comput.* **2012**, *8*, 3314–3321. [\[CrossRef\]](#)

**Disclaimer/Publisher's Note:** The statements, opinions and data contained in all publications are solely those of the individual author(s) and contributor(s) and not of MDPI and/or the editor(s). MDPI and/or the editor(s) disclaim responsibility for any injury to people or property resulting from any ideas, methods, instructions or products referred to in the content.